Compound Synthesis

Supplemental Figure 1 depicts the synthesis of FAPI-19 and the route to the following derivatives.

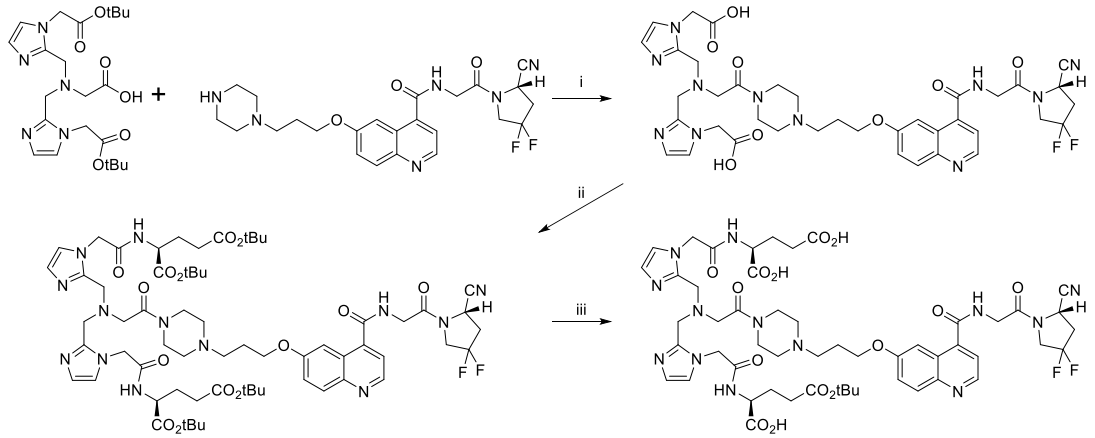

Supplemental Figure 1. Exemplary synthesis of FAPI-29 via FAPI-19. i) HBTU, HOBt, DIPEA then 2.5% TfOH in TFA/MeCN 4:1; ii) HBTU, HOBt, DIPEA, H-Glu(tBu)-OtBu; iii) 2.5% TfOH in TFA/MeCN 4:1.

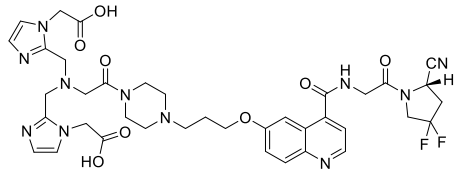

FAPI-19

1.09 mg (1.86 µmol) of (*S*)-*N*-(2-(2-cyano-4,4-difluoropyrrolidin-1-yl)-2-oxoethyl)-6-(3-(4-*tert*-butoxycarbonylpiperazin-1-yl)-1-propoxy)quinoline-4-carboxamide were treated with 100 µL trifluoroacetic acid/acetonitrile 4:1 for 15 min and precipitated after removal of the solvents. The precipitate was reacted with 2.74 mg (5.91 µmol) bis((1-(2-(*tert*-butoxy)-2-oxoethyl)-1H-imidazol-2-yl)methyl)glycine, 2.13 mg (5.62 µmol) HBTU and 2.5 µL DIPEA in 150 µL dimethylformamide. After HPLC purification and solvent removal the residue was treated with 200 µL of 2.5% trifluoromethanesulfonic acid in trifluoroacetic acid/acetonitrile 4:1. After precipitation with diethyl ether and HPLC purification 1.06 mg (1.29 µmol; 70%) of the title compound were obtained.

LC-MS R_t 8.91 min, m/z 820.2933 $[M+H]^+$

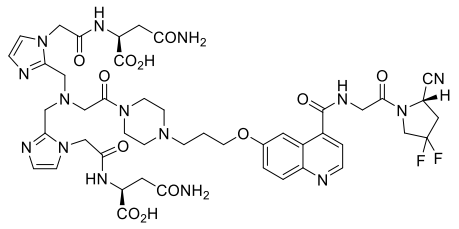

FAPI-28

1 µL (0.74 mg; 5.73 µmol) DIPEA was added to a solution of 0.95 mg (1.16 µmol) FAPI-19, 0.42 mg (3.14 µmol) HOBt and 1.10 mg (2.89 µmol) HBTU in 50 µL DMF. After 10 min 2.30 mg (5.34 µmol) H-Asn(Trt)-OtBu were added and reacted for 120 min. The *tert*-butyl protecting groups were removed by 100 µL 2.5% trifluoromethanesulfonic acid in trifluoroacetic acid/acetonitrile 4:1 after HPLC-purification and freeze-drying. 0.79 mg (0.75 µmol; 65%) were obtained after a final HPLC-purification and freeze-drying.

LC-MS R_t 9.23 min, m/z 524.7100 $[M+2H]^{2+}$

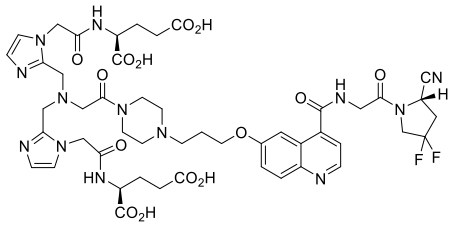

FAPI-29

0.81 mg (0.75 µmol; 65%) were obtained analogous to FAPI-28.

LC-MS R_t 9.25 min, m/z 1078.4109 $[M+H]^{+}$

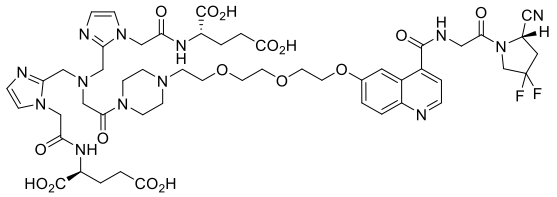

FAPI-33

0.64 mg (0.55 µmol; 60%) were obtained analogous to FAPI-28.

LC-MS R_t 9.85 min, m/z 1152.4493 $[M+H]^{+}$

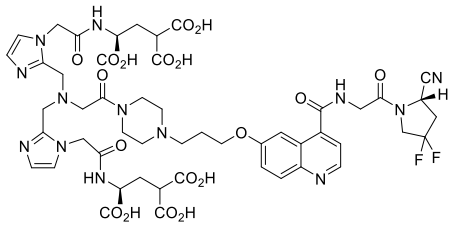

FAPI-34

1.01 mg (0.87 µmol; 52%) were obtained analogous to FAPI-28.

LC-MS R_t 8.87 min, m/z 583.6988 $[M+2H]^{2+}$

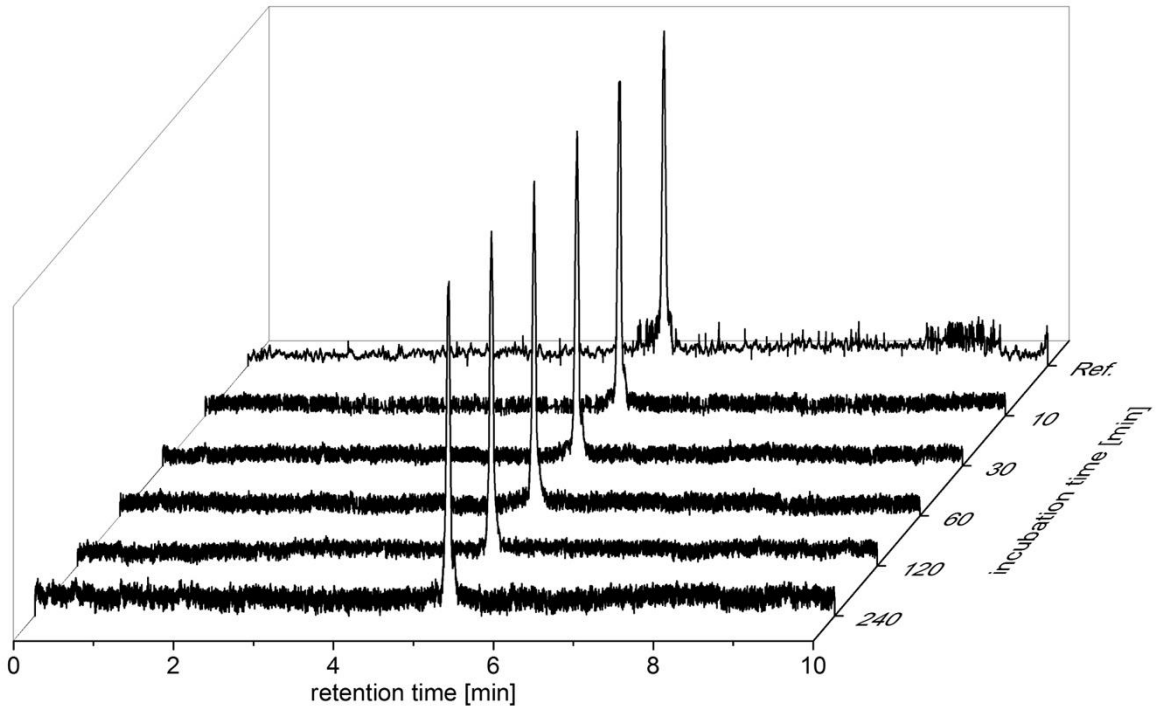

Supplemental Figure 2: Stability of ^{99m}Tc-FAPI-34 in human serum. Samples were precipitated after the indicated time points and the supernatant subjected to radio-HPLC analysis using a linear gradient from 0 to 50 % acetonitrile, containing 0.1 % TFA over 10 min. Neither free radioactivity nor peaks with different retention time than the reference peak were observed confirming the stability against degradation in human serum.

	logP	percent protein bound
^{99m}Tc-FAPI-19	**-1.48**	**96**
^{99m}Tc-FAPI-28	**-1.68**	**97**
^{99m}Tc-FAPI-29	**-1.68**	**97**
^{99m}Tc-FAPI-33	**-1.60**	**95**
^{99m}Tc-FAPI-34	**-1.54**	**98**
^{99m}Tc-FAPI-43	**-1.13**	**98**

Supplemental Table 1. The pharmacokinetic parameter plasma protein binding was determined by ultrafiltration (Amicron Ultra 0.5 mL; 10 kDa) of a serum sample incubated with the radioactive tracer

followed by measurement of the radioactivity in the filtrate and the spinfilter. The physicochemical parameter log P were determined for a selection of six technetium labeled compounds following the procedure of Wilson *et al*. (*1*).

%AD/10^6 cells	Cell-bound fraction (1 h)	Internalized fraction (1 h)	Cell-bound fraction (4 h)	Internalized fraction (4 h)
FAPI-19	0.54±0.02	35.59±1.68	0.54±0.01	37.81±0.39
FAPI-27	1.23±0.23	10.9±0.25	1.34±0.02	12.65±0.62
FAPI-28	0.76±0.03	29.37±0.5	1.9±0.22	36.2±1.05
FAPI-29	1.16±0.09	33.26±2.14	1.6±0.12	36.9±2.56
FAPI-33	1.16±0.26	41.65±2.21	2.13±0.19	44.33±1.32
FAPI-34	0.94±0.14	32.07±0.33	1.86±0.23	39.47±1.4
FAPI-43	0.43±0.04	25.77±1.12	0.46±0.03	28.05±1.14

Supplemental Table 2. Cell-bound (glycin fraction) and internalized activity (lysed fraction) of HT-1080-FAP cells exposed to ^{99m}Tc labeled FAPI derivatives for 1 h and 4 h (%AD/10^6 cells+SD).

FAPI-19 %AD/10^6cells	10 min	60 min
HEK-muFAP	26.13±0.84	36.13±2.23
HEKCD26	0.13±0.01	0.19±0.02

Supplemental Table 3. Binding of ^{99m}Tc-FAPI-19 against HEK cells transfected with murine FAP (HEK-muFAP) or human CD26 (HEKCD26).

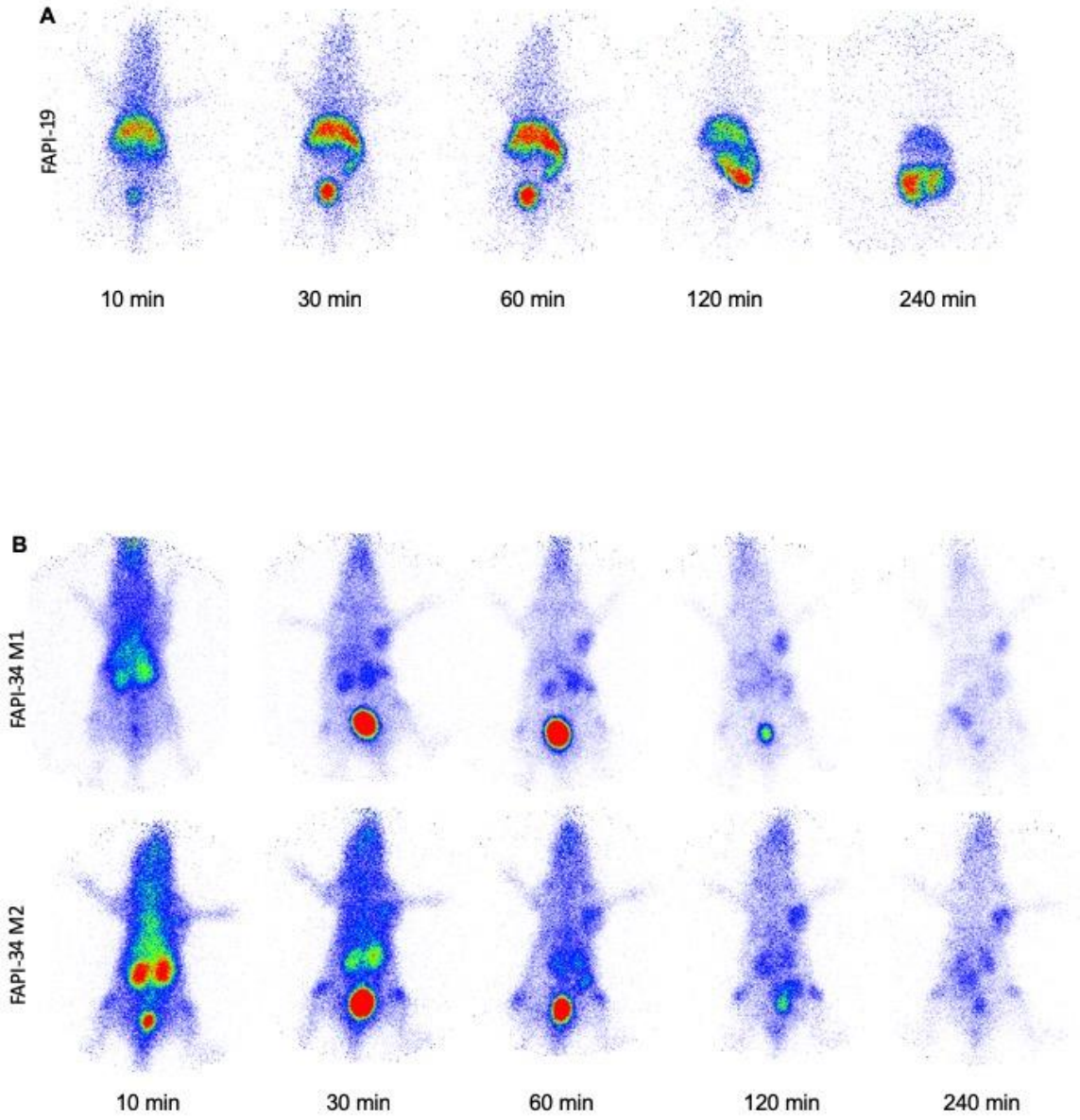

Supplemental Figure 3. Time course of planar scintigraphy with ^{99m}Tc-labeled (A) FAPI-19 and (B) FAPI-34 (two mice) in HT-1080-FAP xenotransplanted mice.

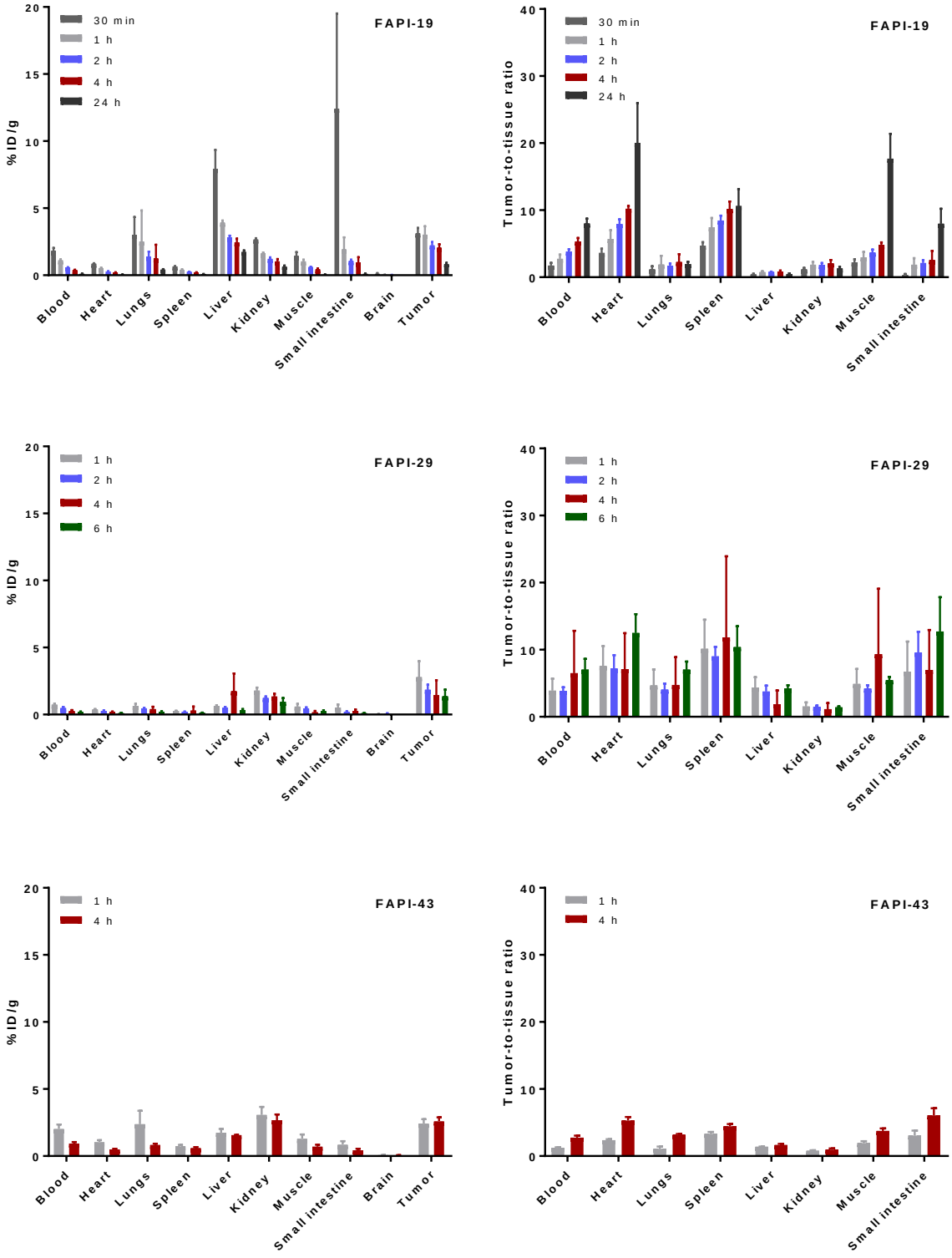

Supplemental Figure 4: Biodistribution (%ID/g; left) and Tumor-to-tissue ratios (right) of ^{99m}Tc-labeled FAPI-19, -29, and -43 (n=3).

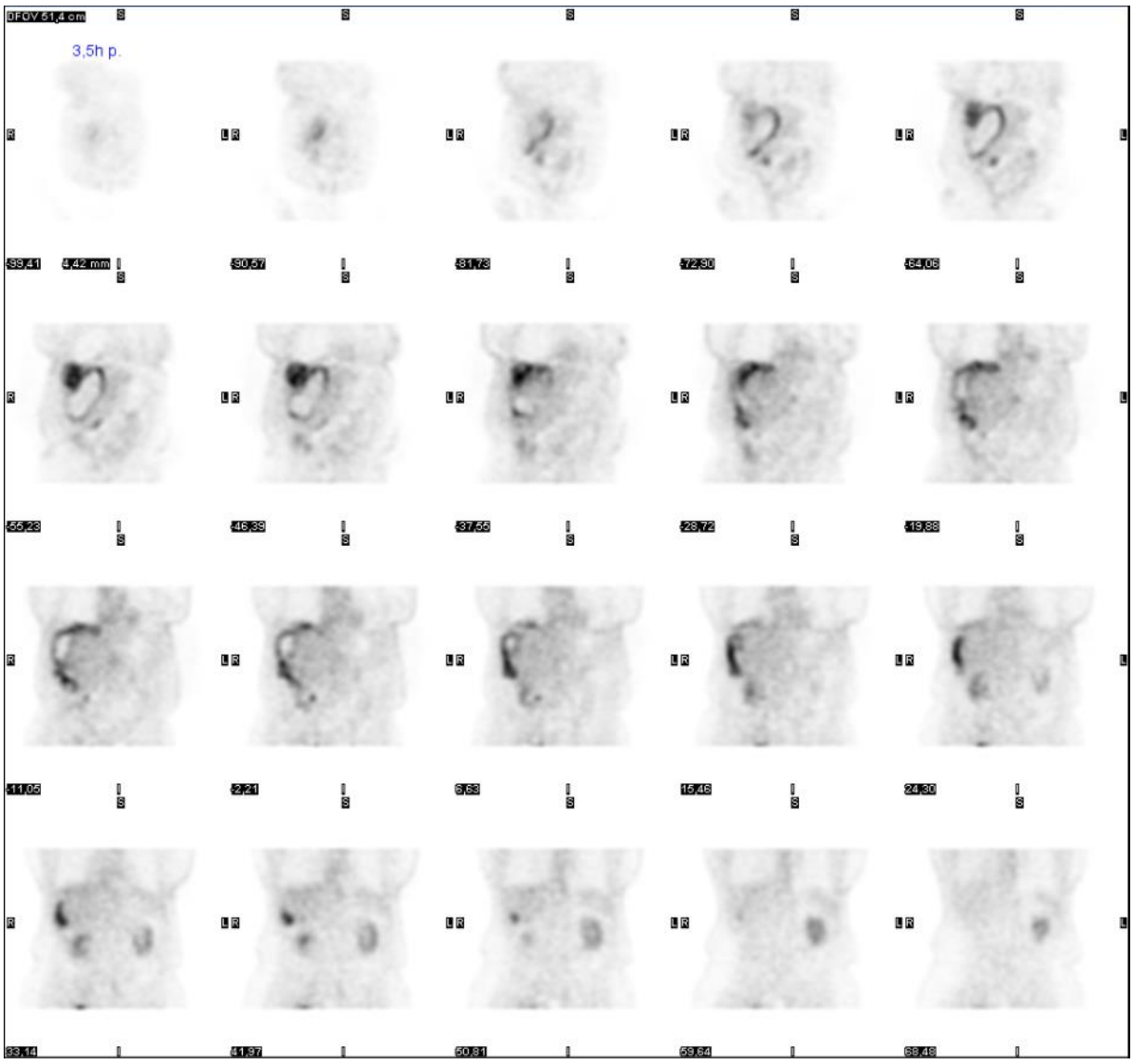
DFOV 51,4 cm
3,5h p.
-99,41
4,42 mm
-90,57
-81,73
-72,90
-64,08
-55,23
-46,39
-37,56
-28,72
-19,88
-11,05
-2,21
6,63
15,46
24,30
33,14
41,97
50,81
59,64
68,48

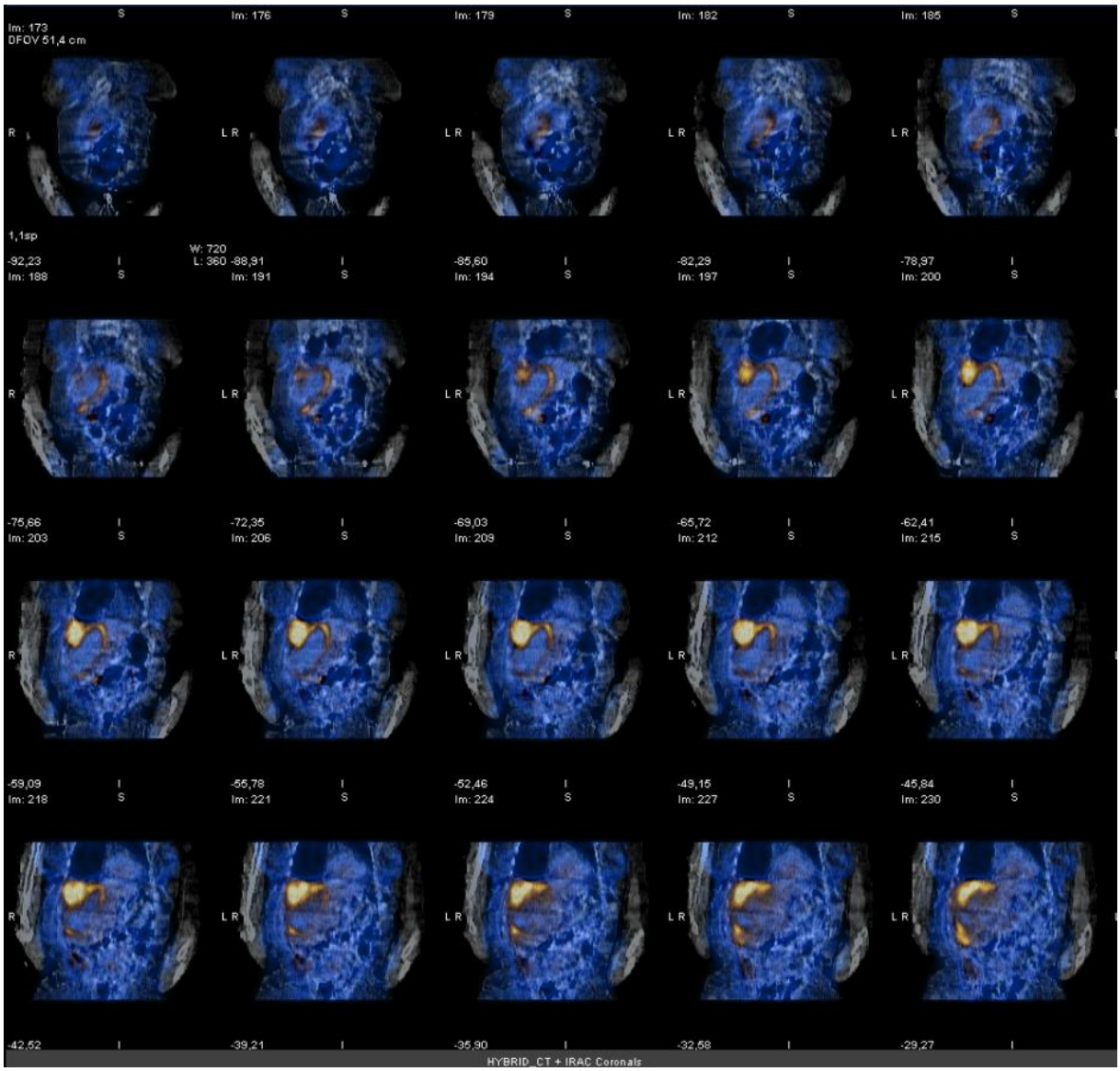
Im: 173
DFOV 51,4 cm
Im: 176
Im: 179
Im: 182
Im: 185
1,1sp
W: 720
L: 360
-92,23
Im: 188
-88,91
Im: 191
-85,60
Im: 194
-82,29
Im: 197
-78,97
Im: 200
-75,66
Im: 203
-72,35
Im: 206
-69,03
Im: 209
-65,72
Im: 212
-62,41
Im: 215
-59,09
Im: 218
-55,78
Im: 221
-52,46
Im: 224
-49,15
Im: 227
-45,84
Im: 230
-42,52
-39,21
-35,90
-32,58
-29,27
HYBRID_CT + IRAC Coronals

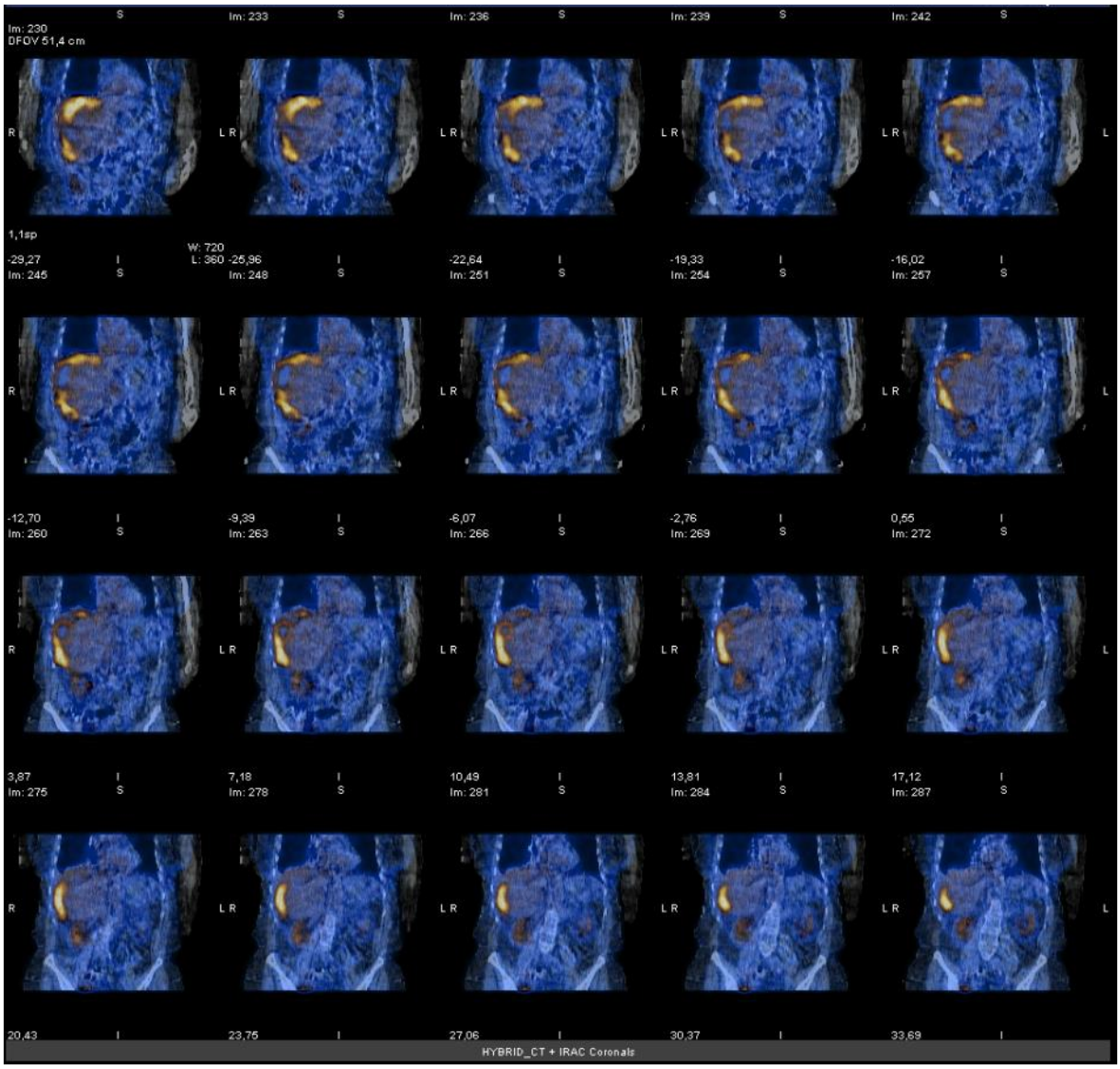

Supplemental Figure 5: Coronal SPECT and fusion SPECT/CT images of the patient with ovarian cancer presented in Figure 5.

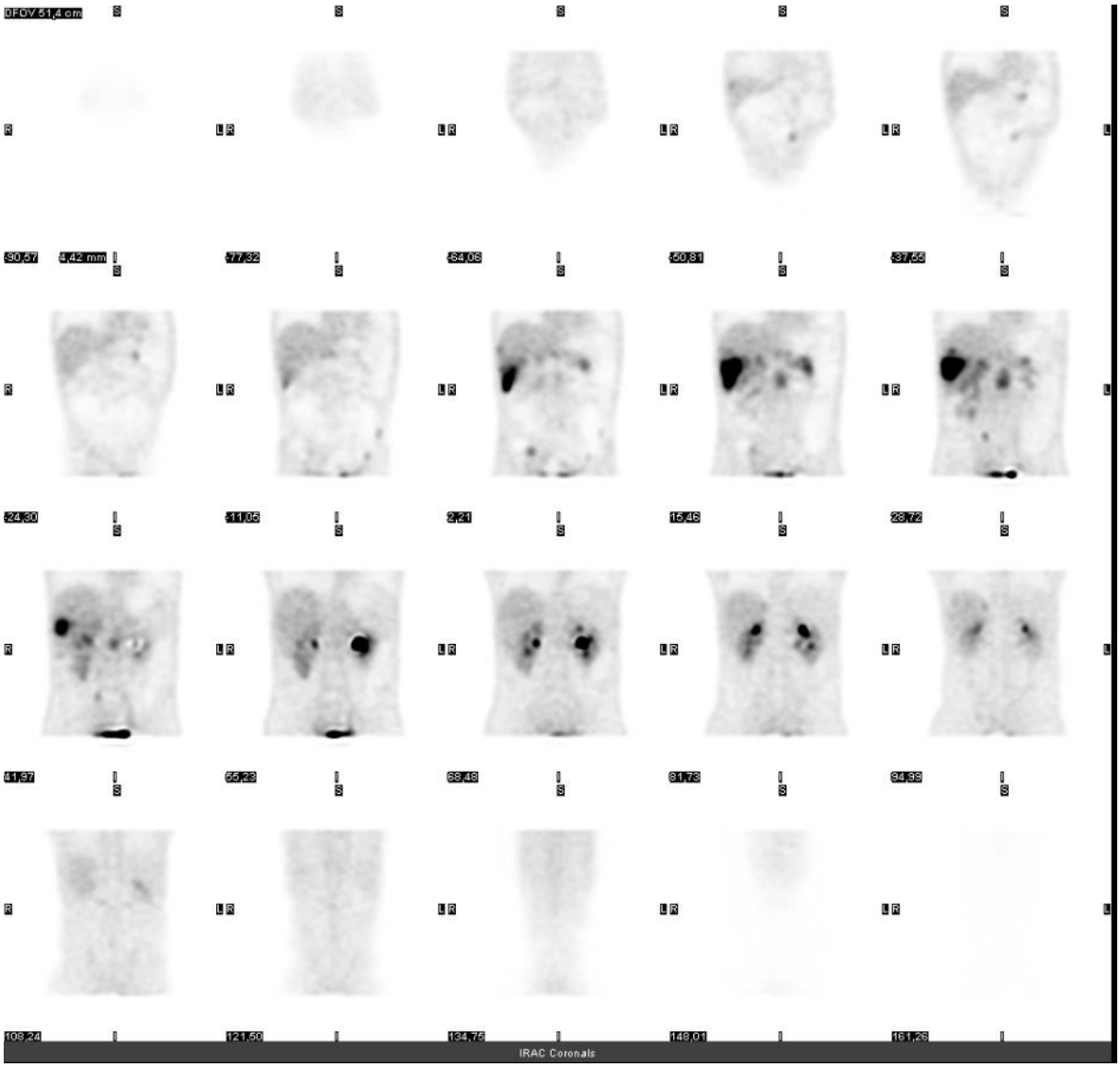
FOV 51,4 cm
-90,57
-77,32
-64,06
-50,81
-37,55
-24,30
-11,06
2,21
15,48
28,72
41,97
55,23
68,48
81,73
94,99
108,24
121,50
134,75
148,01
161,26
IRAC Coronals

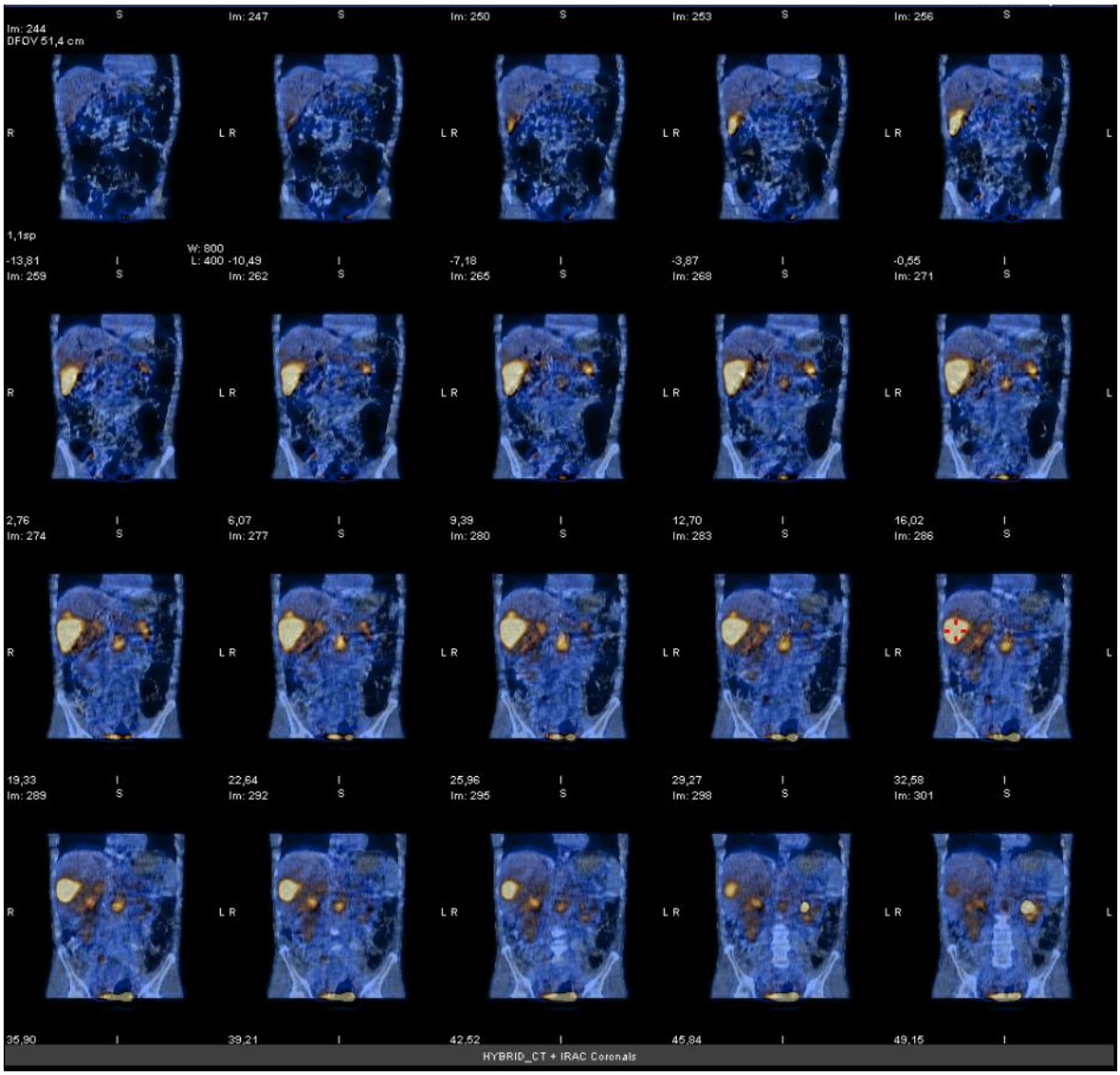

Supplemental Figure 6: Coronal SPECT and fusion SPECT/CT images of the patient with pancreatic cancer presented in Figure 6.

1. Wilson AA, Jin L, Garcia A, DaSilva JN, Houle S. An admonition when measuring the lipophilicity of radiotracers using counting techniques. *Applied Radiation and Isotopes.* 2001;54:203-208.